# Fermi-Löwdin-orbital self-interaction correction using the optimized-effective-potential method within the Krieger-Li-Iafrate approximation

Carlos M. Diaz [*], Tunna Baruah [†] and Rajendra R. Zope [‡]

*Department of Physics, University of Texas at El Paso, El Paso, Texas 79968, USA*

The Perdew-Zunger self-interaction correction (PZ-SIC) offers a route to remove self-interaction errors on an orbital-by-orbital basis. A recent formulation of PZ-SIC by Pederson, Ruzsinszky, and Perdew proposes restricting the unitary transformation to localized orbitals called Fermi-Löwdin orbitals. This formulation, called the FLOSIC method, simplifies PZ-SIC calculations and was implemented self-consistently using a Jacobi-like (FLOSIC-Jacobi) iteration scheme. In this work we implement the FLOSIC approach using the Krieger-Li-Iafrate (KLI) approximation to the optimized effective potential. We compare the results of the present FLOSIC-KLI approach with the FLOSIC-Jacobi scheme for atomic energies, atomization energies, ionization energies, barrier heights, polarizability of chains of hydrogen molecules, etc., to validate the FLOSIC-KLI approach. The FLOSIC-KLI approach, which is within the realm of Kohn-Sham theory, predicts smaller energy gaps between frontier orbitals due to the lowering of eigenvalues of the unoccupied orbitals. Results show that atomic energies, atomization energies, ionization energy as an absolute of highest occupied orbital eigenvalue, and polarizability of chains of hydrogen molecules between the two methods agree within 2%. Finally the FLOSIC-KLI approach is used to determine the vertical ionization energies of water clusters.

## I. INTRODUCTION

The Kohn-Sham (KS) formulation of the density functional theory (DFT) is an exact theory widely used in chemical physics, materials science, and condensed matter physics [1]. Its practical usage requires approximations to the exchange-correlation functional whose accuracy and complexity determine the accuracy and efficiency of the study. As there is no systematic way to improve upon the accuracy of exchange-correlation approximations, a large number of density functional approximations (DFAs) have been proposed [2,3]. Practically, all these functionals suffer from self-interaction error (SIE) which has restricted the universal application of DFT. The SIE has been attributed to the problem of excessive delocalization of electrons, low reaction barrier heights, overestimation of eigenvalues of occupied orbitals, overestimation of polarizabilities of molecular chains, underestimation of band gaps, etc. In KS-DFT, when the exchange-correlation functional is approximated, the self-Coulomb energy included in the expression of Coulomb energy does not get fully canceled by the self-exchange in the approximate exchange-correlation functional. The residual left is the self-interaction energy. For example, for the hydrogen atom or one-electron densities $\rho_{i\sigma}$ of spin $\sigma$ the sum of Coulomb energy $E_H$ and exchange-correlation $E_{xc}$ is

$$E_H + E_{xc} = \frac{1}{2} \iint d^3r\, d^3r' \frac{\rho_{i\sigma}(\vec{r})\rho_{i\sigma}(\vec{r}')}{|\vec{r} - \vec{r}'|} + E_{xc}[\rho_{i\sigma}] = \delta.$$
(1)

For the exact functional $\delta = 0$. For approximate functionals, $\delta$ is nonzero and represents the self-interaction error for that functional for the one-electron density.

Several approaches have been proposed to remove the SIE explicitly [4–15]. Early approaches [4,5] used orbitalwise schemes to eliminate the SIE but used functionals related to Slater's X$\alpha$ method [16]. More common approaches that mitigate SIE include hybrid functionals, which mix Hartree-Fock exchange using various criteria [17–20]. A large literature on the hybrid functionals that were introduced by Becke [17] exist, but these approaches are not entirely self-interaction free and are challenging for extended systems.

### A. Perdew-Zunger SIC

In 1981, Perdew and Zunger (PZ) [21] proposed a method to remove the one-electron SIE in an orbitalwise fashion. This method is the most common approach to explicitly remove the SIE. The PZ self-interaction correction (PZ-SIC) provides the exact cancellation for one-electron self-interaction (SI), but not necessarily for many-electron SI [22]. In the PZ-SIC method [21], the orbitalwise SIC to the total energy is

$$E^{\text{SIC}} = -\sum_{i\sigma}^{N_{\text{occ}}} \left( U[\rho_{i\sigma}] + E_{xc}^{\text{DFA}}[\rho_{i\sigma}, 0] \right).$$
(2)

Here, $U[\rho_{i\sigma}]$ and $E_{xc}^{\text{DFA}}[\rho_{i\sigma}, 0]$ are the Coulomb and exchange-correlation energy of the $i$th occupied orbital, $\sigma$

[*]cmdiaz6@utep.edu
[†]tbaruah@utep.edu
[‡]rzope@utep.edu

is the spin index, $N_{occ}$ is the number of occupied orbitals, and $\rho_{i\sigma}$ is the orbital electron density. It is obvious from Eq. (2) that the PZ-SIC corrections make the DFA exact for any one-electron density. The SIC should vanish for the exact functional. It is unclear if PZ-SIC satisfies this condition. The exact functional is valid only for ground state densities while the SIC using the PZ-SIC method is obtained on an orbital-by-orbital basis, that is, using orbital densities which are noded [23]. The total energy with the PZ-SIC method is given by $E = E^{KS} + E^{SIC}$. In atomic units, $E^{KS}$ is given by

$$E^{KS} = \sum_{i\sigma} \langle \psi_{i\sigma} | -\frac{\nabla^2}{2} | \psi_{i\sigma} \rangle + \int d^3 r \, \rho(\vec{r}) v_{ext}(\vec{r})$$
$$+ \frac{1}{2} \iint d^3 r \, d^3 r' \frac{\rho(\vec{r})\rho(\vec{r}')}{|\vec{r} - \vec{r}'|} + E_{xc}[\rho_\uparrow, \rho_\downarrow]. \quad (3)$$

Here, $v_{ext}$ is the external potential and $\rho = \rho_\uparrow + \rho_\downarrow = \sum_\sigma \rho_\sigma = \sum_{i,\sigma} f_{i\sigma} |\psi_{i\sigma}|^2$ is the electron density, where $f_{i\sigma}$ is the occupation of the $\psi_{i\sigma}$ orbital. Atomic units are used throughout this article unless specified explicitly.

The SI corrected potential seen by an electron in the $i$th orbital in the PZ-SIC method is

$$v_{eff}^{i\sigma}(\vec{r}) = v_{ext}(\vec{r}) + \int d^3 r' \frac{\rho(\vec{r}')}{|\vec{r} - \vec{r}'|} + v_{xc}^\sigma(\vec{r})$$
$$- \left\{ \int d^3 r' \frac{\rho_{i\sigma}(\vec{r}')}{|\vec{r} - \vec{r}'|} + v_{xc}^{i\sigma}(\vec{r}) \right\}. \quad (4)$$

Here, the second term is the Coulomb potential due to the electrons and $v_{xc}$ is the exchange-correlation potential (of DFA). The last two terms in the curly bracket constitute the SIC potential for the $i$th orbital $v_{i\sigma}^{SIC} = -\{v_C^{i\sigma} + v_{xc}^{i\sigma}\}$, composed of the self-Coulomb and self-exchange-correlation potentials. Unlike in the standard KS equations, the potential in Eq. (4) is orbital dependent. This orbital dependence complicates the solution of one-electron equations. For atoms where the KS orbitals are localized, PZ-SIC provides finite SIC. However, the method is not size extensive if the KS orbitals are used. The Kohn-Sham orbitals are delocalized for a system made up of a collection of atoms with large separation between them. These delocalized KS orbitals give vanishing SIC correction if used in the PZ-SIC method. For extended systems the delocalized KS orbitals are normalized over the entire volume of the solid and hence orbital-dependent quantities in Eq. (2) approach zero for such systems. The SIC can be made size extensive by using localized orbitals, which can be obtained from KS orbitals by unitary transformation.

Pederson, Heaton, and Lin implemented such a SIC scheme and demonstrated the first PZ-SIC calculation for molecules [24]. In the 1980s, Lin's group at Wisconsin used a localization approach to implement the PZ-SIC method [24–27]. The orbital-dependent Coulomb and exchange-correlation energies and potentials in Eq. (4) are computed using local orbitals. The localization approach by Pederson and coworkers requires that the local orbitals that minimize total energy must satisfy Pederson's localization equations given here:

$$\langle \phi_i | H_i - H_j | \phi_j \rangle = \lambda_{ji}^i - \lambda_{ij}^j = 0. \quad (5)$$

Here $H_i$ is the orbital-dependent Hamiltonian, $\phi$ are the localized orbitals obtained by unitary transformation of the KS orbitals $\psi$, and $\lambda$ is the Lagrangian multiplier introduced to maintain the orthogonality constraint. When the total energy is at variational minimum the Lagrangian multiplier matrix is symmetric.

The variational minimization of PZ-SIC energy requires satisfying $N(N-1)/2$ localization equations where $N$ is the number of occupied orbitals. In 2014, Pederson and coworkers used Löwdin orthogonalized Fermi orbitals (FLOs) in the PZ-SIC method. The PZ-SIC using FLOs reduces the number of unknown parameters needed to describe the unitary transformation and reduce the number of constraints from $N^2$ to $3N$. Before closing this section we note that a localizing transformation can also be incorporated in the Kohn-Sham formalism using the optimized effective potential (OEP) method as shown by Körzdörfer and coworkers [28]. This generalized OEP method is also invariant under unitary transformation of the orbitals. Below we briefly describe the details of the PZ-SIC using FLOs.

### B. Fermi-Löwdin orbital SIC (FLOSIC)

Recently, Pederson, Ruzsinszky, and Perdew [29] introduced a unitary invariant implementation of PZ-SIC using Fermi-Löwdin orbitals [30,31] called the FLOSIC method. FLOSIC has been used interchangeably with PZ-SIC earlier, but FLOs can also be used in other variants of SIC including OSIC [32], SOSIC [33], and recently introduced local scaling SIC [14] methods. FLOSIC makes use of localized Fermi orbitals (FOs) $F_{i\sigma}$ which are defined by the transformation of KS orbitals as

$$F_{i\sigma}(\vec{r}) = \frac{\sum_\alpha \psi_{\alpha\sigma}^*(\vec{a}_{i\sigma}) \psi_{\alpha\sigma}(\vec{r})}{\sqrt{\sum_\alpha |\psi_{\alpha\sigma}(\vec{a}_{i\sigma})|^2}}. \quad (6)$$

Here, $\vec{a}_{i\sigma}$ are points in space called Fermi-orbital descriptors (FODs). Neglecting the spin index, the above equation can be rewritten as

$$F_i(\vec{r}) = \sum_\alpha^{N_{occ}} F_{i\alpha} \psi_\alpha = \frac{\rho(\vec{a}_i, \vec{r})}{\sqrt{\rho(\vec{a}_i)}}, \quad (7)$$

where the transformation matrix $F_{i\alpha}$ is defined as

$$F_{i\alpha} = \frac{\psi_\alpha^*(\vec{a}_i)}{\sqrt{\rho(\vec{a}_i)}}. \quad (8)$$

The FOs are normalized but are not orthogonal. They are orthogonalized using the Löwdin orthogonalization method to generate the Fermi-Löwdin orbitals (FLOs) $\phi_{i\sigma}$. Optimal FOD positions are found using gradients of the energy with respect to FOD positions using minimization procedures analogous to geometry optimizations [34,35]. A number of studies have been conducted using the FLOSIC method [14,33,36–57].

### C. Self-consistency in FLOSIC

Two routes have been used to implement orbital-dependent functionals. The first one is the generalized Kohn-Sham scheme [58] that is widely used to implement hybrid functionals which contain orbital-dependent Hartree-Fock exchange. This approach lies outside of the traditional Kohn-Sham scheme with multiplicative effective potentials. Within the

Kohn-Sham scheme, orbital-dependent functionals are implemented using the optimized effective potential (OEP) method [59,60].

The PZ-SIC method can also been implemented using the OEP method. In the OEP method total energy is minimized with respect to a local-multiplicative potential [59,60]. This results in integral equations that are very complex and computationally demanding to solve. Typically the OEP solution is obtained using simplifications proposed by the Krieger, Li, and Iafrate (KLI) [61]. A few implementations of the PZ-SIC method using the KLI-OEP have been reported [28,61–66]. For more details about the OEP-PZ-SIC method and its comparison to the non-OEP approach we refer the interested reader to Ref. [28].

Previous implementations of self-consistent FLOSIC used an approach related to Jacobi rotations [37]. In this approach, an approximate Hamiltonian is first constructed as

$$\tilde{H}_{mn\sigma} = \langle \phi_{m\sigma} | H_\sigma^{\text{KS}} + v_{i\sigma}^{\text{SIC}} | \phi_{n\sigma} \rangle, \tag{9}$$

where $H_\sigma^{\text{KS}}$ is the traditional KS Hamiltonian. (See Ref. [37] for more details.) The FLOs and the unoccupied virtual orbitals are made orthogonal through pairwise Jacobi rotations which are carried out iteratively until the matrix elements for the $i$th-orbital Hamiltonian between $\phi_i$ and a virtual orbital vanishes. Alternative schemes such as a unified Hamiltonian [25,54,67] and a generalized-Slater scheme in real space [56] have also been used.

The purpose of this work is to introduce self-consistency in the FLOSIC method using the OEP-KLI approximation. We refer to this implementation as FLOSIC-KLI. We compare the results obtained using FLOSIC-KLI for large number of properties against the Jacobi-rotation approach to self-consistency (FLOSIC-Jacobi) as well as to the experimental values. We also use the present implementation to study the vertical ionization energies of water clusters containing 20 to 30 water molecules. In Sec. II A we describe the FLOSIC-KLI equations. In Sec. III we present results for atomic energies and highest occupied orbital (HOO) eigenvalues as well as total energies and atomization energies of molecules and compare against the self-consistent FLOSIC-Jacobi approach as implemented in the FLOSIC code.

## II. THEORY AND COMPUTATIONAL DETAILS

### A. FLOSIC-KLI equations

The present implementation of PZ-SIC using FLOSIC-KLI closely follows that of Patchkovskii, Autschbach, and Ziegler [63]. In the KLI approximation, the orbital-dependent potential of the PZ-SIC equation (Eq. [4]) is replaced by

$$v_{\text{eff}}^\sigma(\vec{r}) = v_{\text{ext}}(\vec{r}) + \int d^3r' \frac{\rho(\vec{r}')}{|\vec{r} - \vec{r}'|} + v_{xc}^\sigma(\vec{r}) + v_{xc,\sigma}^{\text{KLI}}(\vec{r}). \tag{10}$$

The KLI contribution to the potential is given by the equations

$$v_{xc,\sigma}^{\text{KLI}}(\vec{r}) = v_{xc,\sigma}^S(\vec{r}) + \sum_{i=1}^{N_\sigma} \frac{\tilde{\rho}_{i\sigma}(\vec{r})}{\rho_\sigma(\vec{r})}(x_{i\sigma} - C_\sigma), \tag{11}$$

$$\tilde{\rho}_{i\sigma}(\vec{r}) = f_{i\sigma} |\phi_{i\sigma}(\vec{r})|^2. \tag{12}$$

In the present formulation, $\phi_{i\sigma}$ are the FLOs (localized orbitals) described in Sec. I B. It has been found that using $\phi_{i\sigma}$ as Kohn-Sham orbitals leads to poor results [62,64]. The leading contribution to the KLI potential is the density-weighted average of the orbital SIC potentials, $v_{xc,\sigma}^S$. This term is similar to the Slater approximation [16] to the average exchange potential and is given as

$$v_{xc,\sigma}^S(\vec{r}) = \sum_{i=1}^{N_\sigma} \frac{\tilde{\rho}_{i\sigma}(\vec{r})}{\rho_\sigma(\vec{r})} v_{i\sigma}^{\text{SIC}}(\vec{r}). \tag{13}$$

The second term in Eq. (11) allows a per-orbital shift in potentials due to the $x_{i\sigma} - C_\sigma$ factor. The magnitudes of the shifts can be determined by enforcing a constraint that the interaction energy between a given localized electron and the shifted SIC potential, $v_{i\sigma}^{\text{SIC}}(\vec{r}) + x_{i\sigma} - C_\sigma$, equals the energy of the electron in the average potential:

$$\int \left[ v_{i\sigma}^{\text{SIC}}(\vec{r}) + x_{i\sigma} - C_\sigma \right] \rho_{i\sigma}(\vec{r}) d\vec{r} = \int v_{xc,\sigma}^{\text{KLI}}(\vec{r}) \rho_{i\sigma}(\vec{r}) d\vec{r}. \tag{14}$$

Substituting $V_{xc,\sigma}^{\text{KLI}}$ from Eq. (11) results in a system of linear equations for $x_{i\sigma}$:

$$\sum_{j=1}^{N_\sigma} (\delta_{ij} f_{i\sigma} - M_{ij}^\sigma) x_{j\sigma} = \bar{v}_{i\sigma}^S - \bar{v}_{i\sigma}^{\text{SIC}}, \quad i = 1, \dots, N_\sigma, \tag{15}$$

where

$$M_{ij}^\sigma = \int \frac{\rho_{i\sigma}(\vec{r}) \rho_{j\sigma}(\vec{r})}{\rho_\sigma(\vec{r})} d\vec{r}, \tag{16}$$

$$\bar{v}_{i\sigma}^S = \int \rho_{i\sigma}(\vec{r}) v_{xc,\sigma}^S(\vec{r}) d\vec{r}, \tag{17}$$

$$\bar{v}_{i\sigma}^{\text{SIC}} = \int \rho_{i\sigma}(\vec{r}) v_{i\sigma}^{\text{SIC}}(\vec{r}) d\vec{r}. \tag{18}$$

From Eqs. (13) and (16)–(18) it follows

$$\sum_{i=1}^{N_\sigma} M_{ij}^\sigma = 1, \tag{19}$$

$$\sum_{i=1}^{N_\sigma} (\bar{v}_{i\sigma}^S - \bar{v}_{i\sigma}^{\text{SIC}}) = 0. \tag{20}$$

In the original KLI approach, the values of the coefficients $x_{i\sigma}$ are chosen to satisfy

$$v_{xc}^{\text{KLI}}(\vec{r}) = v_{xc,\sigma}^S(\vec{r}) + \sum_{i=1}^{N_\sigma} \frac{\rho_{i\sigma}(\vec{r})}{\rho_\sigma(\vec{r})} (\bar{v}_{xc,i\sigma}^{\text{KLI}} - \bar{v}_{i\sigma}^{\text{SIC}}), \tag{21}$$

where

$$\bar{v}_{xc,i\sigma}^{\text{KLI}}(\vec{r}) = \int \rho_{i\sigma}(\vec{r}) v_{xc,\sigma}^{\text{KLI}}(\vec{r}) d\vec{r}. \tag{22}$$

In the limit as $r \to \infty$, $\rho_\sigma$ can be expected to be dominated by the highest occupied molecular orbital (HOMO), $\rho_\sigma^{\text{HOMO}}$. In this limit, it follows that

$$v_{xc,\sigma}^{\text{DFA}}(\vec{r}) + v_{xc}^{\text{KLI}} \to -\frac{1}{r} + x_\sigma^{HOMO} - x_\sigma. \tag{23}$$
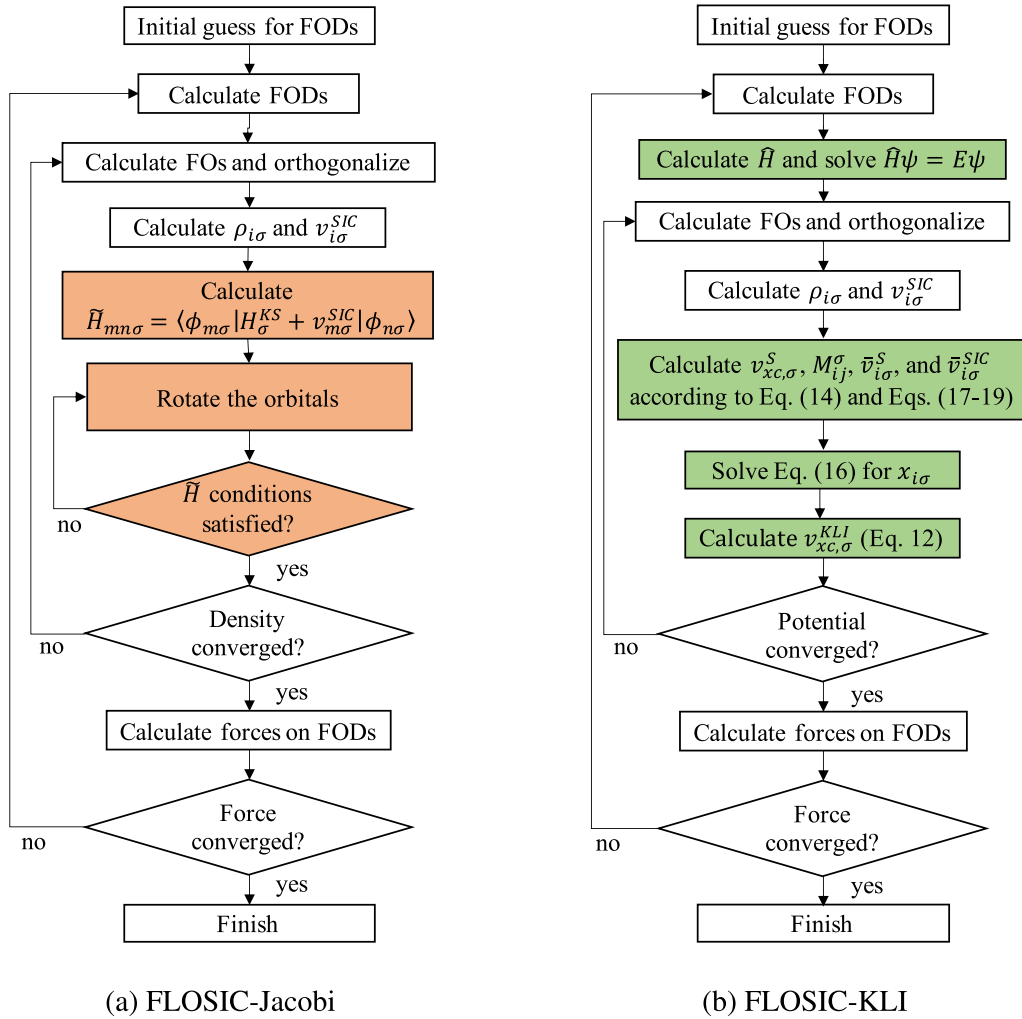
FIG. 1. SCF diagrams of FLOSIC-Jacobi and FLOSIC-KLI schemes. Differences highlighted in red for FLOSIC-Jacobi and green for FLOSIC-KLI.

Equation (11) is identical to the KLI-OEP expression if $C_\sigma$ is chosen as $C_\sigma = x_\sigma^{\text{HOMO}}$. For other choices of $C_\sigma$, the potentials differ by a constant. Patchkovskii *et al.* [63] note difficulties in defining the HOMO in molecular calculations and find a choice of $C_\sigma = \min(x_{i\sigma})$ to give favorable convergence properties. In our calculations, we find using $C_\sigma = \max(x_{i\sigma})$ to give orbital energies comparable to original FLOSIC-Jacobi calculations and favorable convergence for most systems tested. Two exceptions were the atomic cases of lithium and sodium, where calculations failed to converge. In these cases, total energies were calculated using $C_\sigma = \min(x_{i\sigma})$. For the two problematic cases of lithium and sodium, calculations can be converged by fixing the orbital occupation. This gives the same total energies as by choosing $C_\sigma = \min(x_{i\sigma})$, but in these cases the lowest unoccupied molecular orbital (LUMO) energy is brought lower than the HOMO, which is of opposite spin. Since orbital eigenvalues are affected by the choice of $C_\sigma$, the HOMO energies for lithium and sodium are not included in errors reported in Sec. III. The steps to solve FLOSIC-KLI equations self-consistently and the difference of the FLOSIC-KLI implementation from the FLOSIC-Jacobi scheme are illustrated in Fig. 1.

### B. Computational details

All of the results presented in this article are calculated with the FLOSIC code [68,69], which is based on the UTEP version of the NRLMOL electronic structure code [70,71]. The FLOSIC code inherits the optimized Gaussian basis sets of NRLMOL [72] and an accurate numerical integration grid scheme [70]. The SIC calculations require a finer mesh as orbital densities are involved in calculation of orbital-dependent potentials. A default NRLMOL mesh for FLOSIC calculation, on average, has 25 000 grid points per atom. This results in integration of charge density that is accurate to the order of $10^{-8}e$. All calculations use the Perdew, Burke, and Ernzerhof (PBE) exchange-correlation functional [73] except for the water clusters. Water cluster calculations were performed using PBE as well as the local spin density approximation (LSDA). For the LSDA correlation, the Perdew-Wang parametrization [74] was used. A self-consistency convergence tolerance of $10^{-6}$ Ha in the total energy was used for all calculations.

FLOSIC calculations require an initial set of trial FOD positions. We use previously reported PBE-optimized FOD positions. These FOD positions were optimized by minimizing the FOD forces [34] until the convergence criteria of

$10^{-6}$ Ha on the FLOSIC total energy was met. FOD positions were not reoptimized for KLI calculations, except for the calculations on hydrogen chains in Sec. IV. We note that this is an additional approximation. The FOD positions depend on the choice of the Hamiltonian and the exchange-correlation approximation. We have examined the effect of this approximation by reoptimizing the FODs for atomic systems within the FLOSIC-KLI scheme. We find that the optimization results in 0.36% change (0.58 millihartrees) in the mean absolute error (MAE) compared to experiment, in each case bringing the results to better agreement with the FLOSIC-Jacobi results. The largest observed change was a 3 millihartree lowering in the case of the fluorine atom, bringing it within 3 millihartrees of the optimized FLOSIC-Jacobi result. We refer to calculations using the Jacobi-rotation approach to self-consistency as FLOSIC-Jacobi and calculations using the KLI approximation as FLOSIC-KLI. A subset of calculations were obtained using only a leading term of the KLI approximation (Eq. [13]) which we refer to as FLOSIC-Slater. The FOD positions for the water clusters were obtained using the fodMC code [75].

### C. Average-density SIC (ADSIC) guess

The iterative solution of KS or PZ-SIC equations requires an initial guess to start the self-consistent field (SCF) cycle. Several choices of initial guess exist. Since its inception in late 1980s, the NRLMOL code (on which the FLOSIC code is based) uses a linear superposition of atomic potentials (SAPs) as an initial guess. The atomic potentials are generated on the fly and a least-squares fit is used to construct initial potentials for molecular systems. Our experience is that this choice has worked well for wide variety of systems. Recently, Lehtola [76] has reviewed the performance of various choices for initial guess to initialize the SCF cycle and has concluded that SAP on average performs better than other choices. Typically in FLOSIC calculations we either start from SAP or from the converged DFA (SIC-uncorrected) KS orbitals. This has worked well but there are cases where starting DFA KS density can have incorrect character, for example when molecules are in dissociation limits. In such case self-consistent FLOSIC calculations can take longer to converge. An alternative if not better initial SAP for SIC calculations can be generated from the self-interaction corrected atomic potentials using a suitable SIC method. We construct the SAP using a simple average-density SIC (ADSIC) scheme [66,77], which is a generalization of the Fermi and Amaldi [78] method. OEP-KLI-SIC can also be used but we have chosen ADSIC due to its simplicity. The KS effective potential in ADSIC exhibits the correct $-1/r$ asymptotic.

In ADSIC, the self-interaction corrections to the Coulomb and exchange-correlation potential are given by

$$V_C^{\mathrm{ADSIC}} = V_C[\rho] - V_C\left[\frac{\rho}{N_e}\right] = V_C \frac{N_e - 1}{N_e} \qquad (24)$$

and

$$V_{xc}^{\mathrm{ADSIC}} = V_{xc}[\rho] - V_{xc}\left[\frac{\rho}{N_e}\right]. \qquad (25)$$

Here, $N_e$ is the number of electrons. This correction can become very small for systems with a large number of electrons, but here we are using it only to generate atomic potentials. In general, we have found that using superposition of ADSIC atomic potentials as an initial guess in the self-consistent FLOSIC calculations usually, but not always, requires fewer iterations to converge than starting from SAP from DFAs or starting from the converged DFA orbitals.

### D. KLI implementation/parallelization

One advantage of the FLOSIC-KLI implementation is that the equations involved are relatively easy to parallelize. The most expensive step in the self-consistent FLOSIC calculation is the determination of orbital-dependent potentials, particularly the Coulomb potential, required to compute the SIC terms. However these potentials are independent of each other and can be easily parallelized. The FLOSIC code, which is parallelized using MPI, adds a second level of parallelization for these calculations. The construction of the Hamiltonian using the Jacobi-like method of Yang, Pederson, and Perdew [37] is harder to parallelize and creates a bottleneck for larger calculations. The present FLOSIC-KLI scheme offers easy parallelization and helps in improving scalability. In the FLOSIC-KLI approach, the SIC potentials and orbital densities are stored to disk after they are computed. Subsequently, each processor reads from file $V^{\mathrm{SIC}}$ and $\rho_i$ and the integrals used to generate $M$, $\bar{v}_{i\sigma}^S$, and $\bar{v}_{i\sigma}^{\mathrm{SIC}}$ [Eqs. (16)–(18)] are then parallelized over batches of grid points.

The contributions from each batch of grid points to the integrals are then reduced across processors. Construction of the $M$ matrix scales as $O(N_e^2)$ and is thus efficiently parallelized. In contrast, the Jacobi-like method scales as $O(N_e N_b^3)$, where $N_b$ is the number of basis functions in a calculation. Since $\rho_i$ which is obtained from the FLO will be localized, we may be able to reduce scaling to $O(N_e)$ by taking advantage of the sparsity of the density. In the subsequent section we compare the FLOSIC-KLI approach against the FLOSIC-Jacobi approach of Yang, Pederson, and Perdew [37] using standard data sets previously employed for assessing the performance of FLOSIC method. We also report new results on the vertical ionization energies of intermediate-size water clusters.

### III. RESULTS

#### A. Atoms: Total energies and eigenvalues

FLOSIC energies for atoms from H–Ar ($Z = 1$–18) are compared against accurate total energies reported by Chakravorty *et al.* [79]. We report the deviation on a per electron basis as $(E - E_{\mathrm{Ref}})/N_e$, where $E$ is the FLOSIC energy and $E_{\mathrm{Ref}}$ is the reference energy. We find that the FLOSIC-KLI results give very close energies compared with the original FLOSIC implementation, with a mean absolute error (MAE) of 0.161 Ha for FLOSIC-KLI compared to 0.158 Ha for FLOSIC-Jacobi. The FLOSIC-Slater calculations perform slightly worse in each case, as shown in Fig. 2, and did not converge for the lithium and sodium atoms. FLOSIC-KLI calculations for these atoms were converged by using the $C_\sigma = \min(x_{i\sigma})$ factor, as detailed in Sec. II A. Neglecting these
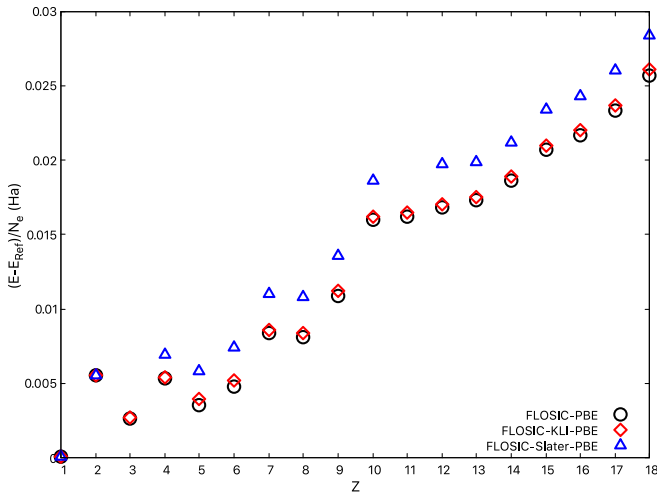
FIG. 2. Atomic total energies (in Ha) for FLOSIC-Jacobi, FLOSIC-KLI, and FLOSIC-Slater compared against the reference values of Ref. [79]. $(E - E_{Ref})/N_e$ is shown, where $N_e$ is the number of electrons.

atoms, FLOSIC-KLI, FLOSIC-Jacobi, and FLOSIC-Slater give a MAE of 0.170, 0.167, and 0.192 Ha, respectively.

The vertical ionization potential (vIP) can be obtained from the negative of the highest occupied orbital (HOO) eigenvalue. For the exact exchange-correlation functionals, they are equal [6,80,81]. For the approximate functionals, the quality of the asymptotic behavior of the exchange functionals determines the accuracy of the HOO as an approximation to the vIP. All semilocal functionals perform poorly in this regard. In Fig. 3 we compare the HOO eigenvalues to experimental ionization potentials (IPs) [82]. Table I shows the MAEs and mean absolute relative errors (MAREs) for the FLOSIC-Jacobi and FLOSIC-KLI approaches, as well as the less accurate FLOSIC-Slater approximation. These results show good agreement between FLOSIC-Jacobi and FLOSIC-KLI, with a difference in MARE of less than 1%. FLOSIC-Slater performs slightly worse with a MARE 3.8% higher than that of FLOSIC-Jacobi.
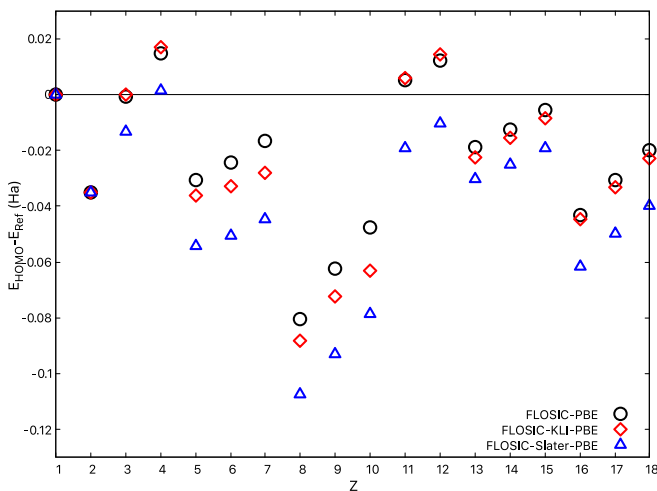


FIG. 3. Error in HOMO eigenvalues (in Ha) compared to experimental IPs [82].

TABLE I. MAE (in Ha) and MARE (%) of HOMO eigenvalues compared to experimental IPs [82]. FLOSIC-Jacobi results from [52].

|  | FLOSIC-Jacobi | FLOSIC-KLI | FLOSIC-Slater |
|---|---|---|---|
| MAE (Ha) | 0.026 | 0.030 | 0.041 |
| MARE (%) | 5.67 | 6.62 | 9.44 |

### B. Atomization energies

FLOSIC-Jacobi and FLOSIC-KLI are also used to calculate the total and atomization energies (AEs) of a set of 37 molecules taken from the G2/97 test set [83]. In addition, we include the six molecules from the AE6 test set [84], as well as HBr, LiBr, NaBr, FBr, and $Br_2$. Most of the geometries were optimized using B3LYP with the 6-31G(2df,p) basis [85]. The geometries for $O_2$, CO, $CO_2$, $C_2H_2$, $Li_2$, $CH_4$, $NH_3$, and $H_2O$ were optimized using the PBE functional and the default NRLMOL basis set. The atomization energy (AE) of a molecule is defined as $AE = \sum_i^{N_{atoms}} E_i - E_{mol} > 0$, where $E_i$ is the energy of individual atoms, $N_{atom}$ is the number of atoms in the molecule, and $E_{mol}$ is the total energy of the molecule. For the AE6 set, we find that FLOSIC-KLI has slightly larger MARE (7.51%) compared to FLOSIC-Jacobi (6.82%).

For the larger set of molecules the average errors in calculated AEs for FLOSIC-Jacobi and FLOSIC-KLI calculations are summarized in Table II. Experimental values are taken from Ref. [82]. The MAREs are 9.67% and 10.00% for FLOSIC-Jacobi and FLOSIC-KLI, respectively. Figure 4 shows a close agreement between two implementations for most systems, except for $F_2$.

Figure 5 plots the differences in total energies between the FLOSIC-Jacobi and FLOSIC-KLI implementations as a function of number of electrons for all atoms and molecules tested. The plot shows a linear behavior, signifying the error per electron to fall within some constant range. When calculating quantities such as AEs, these differences cancel out.

## IV. POLARIZABILITY OF $H_2$ CHAINS

Most semilocal functionals perform poorly in predicting the response of charge distributions to electric fields for molecular chains and polymers [86–90]. The polarizabilities predicted by semilocal functionals are severely overestimated. However, recent work by Aschebrock and Kümmel shows that meta-GGA functionals constructed by considering KS-potential-related properties such as the derivative discontinuity and its density response can provide an accurate description of polarizabilities [91]. The chains of hydrogen molecules have been extensively used as model systems

TABLE II. Atomization energies for the set of molecules featured in Fig. 4. MAE (kcal/mol) and MARE (%) are shown.

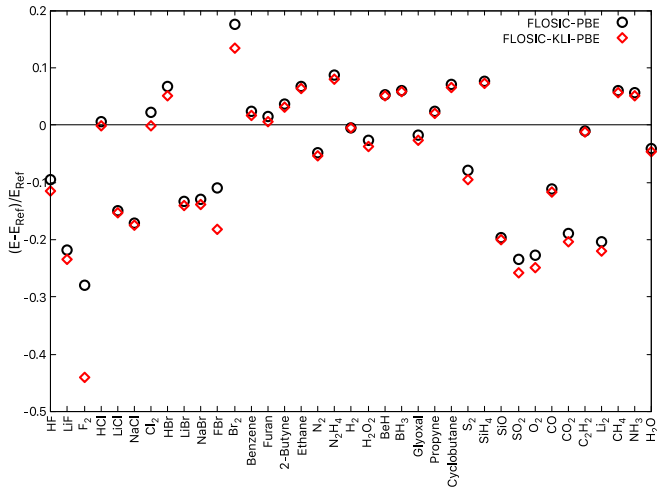|  | FLOSIC-Jacobi | FLOSIC-KLI |
|---|---|---|
| MAE (kcal/mol) | 84.29 | 83.32 |
| MARE (%) | 9.67 | 10.00 |

FIG. 4. Relative error $(E - E_{\text{Ref}})/E_{\text{Ref}}$ of atomization energies of molecules compared against the reference experimental values found in Ref. [82].

to examine performance of DFAs in predicting the electric response of molecular chains [53,86,92–99]. The overestimation of polarizabilities has been understood as a result of a missing field-counteracting term in the response part of the XC potentials of semilocal functionals [86,92]. Here, we use hydrogen chains to examine how well FLOSIC-KLI compares with FLOSIC-Jacobi for the polarizabilities of these systems. For this purpose we use the *finite-field* method with an electric field of $h = 1.0 \times 10^{-3}$ a.u. The polarizability is calculated using a second-order central finite difference approach. The $z$ component of the polarizability $\alpha_{zz}$ is calculated as

$$\alpha_{zz} = \frac{d\mu_z}{dF_z} = \frac{d^2E}{dF_z^2} = \frac{E(-h) - 2E(0) + E(h)}{h^2}, \quad (26)$$

where $h$ is the $z$ component of the electric field.

Table III shows the calculated polarizabilities for $H_n$ chains comparing PBE, FLOSIC-Jacobi, and FLOSIC-KLI (see also Fig. 6). We constructed linear chains of hydrogen atoms by

TABLE III. Polarizabilities $\alpha_{zz}$ of $H_2$ chains (in a.u.). MP4 and CCSD values from Ref. [96]. Mean absolute relative error (MARE) relative to CCSD(T) calculations for $H_{4-12}$.

| Method | $H_4$ | $H_6$ | $H_8$ | $H_{12}$ | $H_{14}$ | $H_{100}$ | MARE (%) |
|---|---|---|---|---|---|---|---|
| PBE | 36.0 | 69.1 | 108.4 | 197.0 | 243.9 | 2600.1 | 43.1 |
| FLOSIC-KLI[a] | 32.1 | 56.8 | 83.6 | 158.7 | 173.7 | 1417.7 | 17.3 |
| FLOSIC-KLI | 32.1 | 59.2 | 88.6 | 158.5 | 180.5 | | 20.1 |
| FLOSIC-Jacobi | 31.2 | 60.3 | 90.5 | 156.9 | 194.8 | | 20.3 |
| MP4 | 29.5 | 51.9 | 75.2 | 127.3 | 155.0 | | 3.3 |
| CCSD(T) | 28.7 | 50.2 | 73.4 | 122.0 | | | |

[a]FOD positions in these calculations are not optimized.

placing hydrogen atoms with alternating distances of 2 and 3 bohrs. Initial FODs were generated by placing a spin-up and spin-down FOD at the midpoint between each bonded $H_2$ molecule. Polarizabilities were then calculated using the initial guess as well as by optimizing FODs using a $10^{-4}$ Ha/bohr convergence criterion. In the case of the $H_{100}$ chain, the FOD positions were not optimized. Table III shows that the polarizabilities calculated using the initial guess of FODs show a mean average error of 2.7% compared to the final optimized calculations, and lie between the FOD-optimized calculations and the MP4 reference calculations.

## V. HOMO-LUMO GAPS

There has been considerable discussion about the interpretation of Kohn-Sham orbital energies as electron removal energies or the differences between the orbital energies as the excitation energies [6,58,80,81,100–117]. Despite these, the density of states from Kohn-Sham calculations is often used to interpret experimental observations. DFAs that have explicit orbital dependence, such as hybrid or meta-GGA functionals, are typically implemented using the generalized Kohn-Sham scheme [58]. The self-consistent implementation of the PZ-SIC method using the Jacobi scheme (FLOSIC-Jacobi)
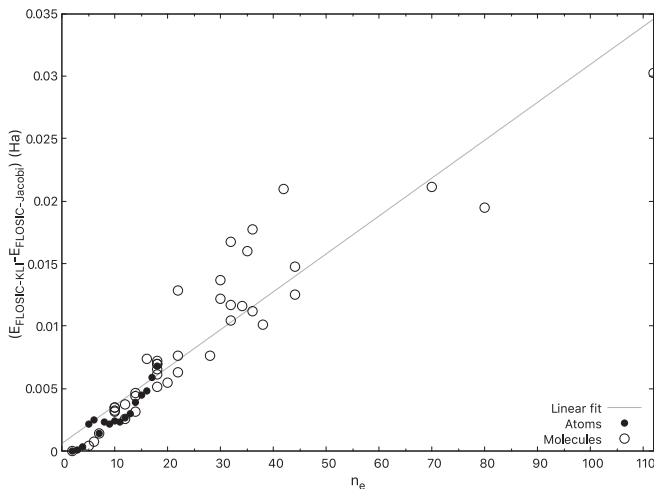


FIG. 5. Difference in total energy (in Ha) between FLOSIC-Jacobi and FLOSIC-KLI calculations as a function of the number of electrons in the system. Linear fit of data shown as solid line.
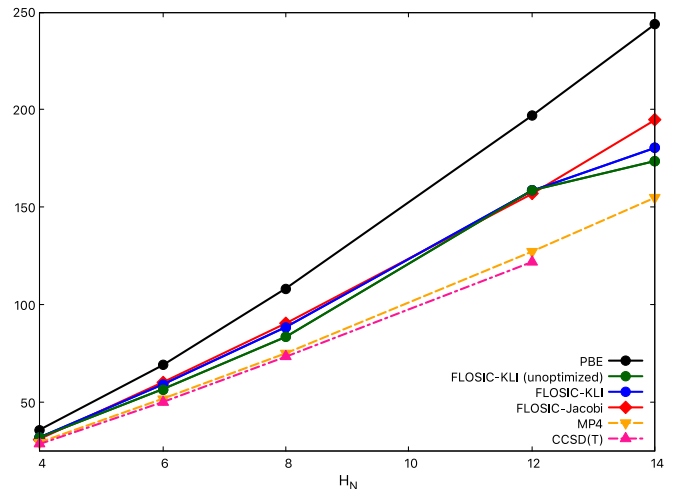


FIG. 6. Polarizabilities $\alpha_{zz}$ of $H_2$ chains (in a.u.) plotted as a function of number of hydrogen atoms. MP4 and CCSD values from Ref. [96].

TABLE IV. HOMO and LUMO eigenvalues for Jacobi and KLI (in eV) along with the difference in HOMO-LUMO gaps. The negative of the HOMO eigenvalues approximate the vertical ionization potentials.

| Molecule | HOMO (eV) | | LUMO (eV) | | Gap Difference |
|---|---|---|---|---|---|
| | FLOSIC-Jacobi | FLOSIC-KLI | FLOSIC-Jacobi | FLOSIC-KLI | |
| HF | −17.82 | −17.55 | −0.53 | −6.28 | −6.02 |
| LiF | −13.20 | −13.44 | −1.32 | −5.28 | −3.72 |
| HCl | −13.43 | −13.47 | −0.90 | −5.59 | −4.66 |
| LiCl | −10.69 | −10.72 | −1.75 | −4.74 | −2.97 |
| NaCl | −10.06 | −10.05 | −2.12 | −5.33 | −3.21 |
| $Cl_2$ | −12.89 | −12.31 | −4.68 | −9.16 | −5.06 |
| HBr | −12.19 | −12.11 | −1.38 | −5.57 | −4.27 |
| LiBr | −9.84 | −9.85 | −1.86 | −4.64 | −2.77 |
| BrF | −12.70 | −12.44 | −4.76 | −9.66 | −5.15 |
| $Br_2$ | −11.67 | −11.19 | −4.92 | −8.84 | −4.40 |
| Benzene | −9.08 | −8.82 | −1.40 | −3.63 | −2.49 |
| Furan | −10.36 | −10.64 | −0.92 | −5.65 | −4.44 |
| 2-Butyne | −11.00 | −10.98 | 0.04 | −4.12 | −4.18 |
| $C_2H_6$ | −14.30 | −14.19 | 0.10 | −4.67 | −4.88 |
| $C_5H_5$ | −1.62 | −1.29 | 4.43 | 3.29 | −1.48 |
| $CN^-$ | −5.17 | −4.79 | 6.78 | 2.11 | −5.06 |
| $N_2$ | −17.24 | −16.15 | −2.05 | −7.44 | −6.49 |
| $BH_3$ | −14.36 | −14.48 | −3.01 | −8.75 | −5.63 |
| Cyclobutane | −13.10 | −13.08 | 0.12 | −4.51 | −4.65 |
| $S_2$ | −10.94 | −11.08 | −4.65 | −7.80 | −3.01 |
| $SiH_4$ | −13.99 | −14.01 | 0.17 | −4.91 | −5.05 |
| SiO | −12.41 | −12.04 | −2.92 | −6.89 | −4.34 |
| $SO_2$ | −14.48 | −14.19 | −4.64 | −9.99 | −5.64 |

is like the generalized KS scheme used for hybrid DFAs or meta-GGAs.

The FLOSIC-KLI method gives a multiplicative effective potential as in the standard KS scheme. As seen in previous sections, these two implementations of the PZ-SIC give total atomic energies, atomization energies, and polarizabilities that agree within 1%–2%. The eigenvalues, especially the eigenvalues of the unoccupied molecular orbitals (LUMOs), in the two approaches are however very different. The FLOSIC-Jacobi LUMOs are essentially the same as those of the uncorrected functional as the Jacobi scheme does not affect the unoccupied orbitals. As can be seen from Table IV and Fig. 7, the FLOSIC-KLI LUMO (and higher unoccupied orbitals) are substantially lowered compared to the FLOSIC-Jacobi LUMO. The calculations also show that the eigenvalues of the core orbitals (especially those of $1s$ orbitals) are destabilized by several eV in the FLOSIC-KLI scheme. Since the HOMO eigenvalues between the FLOSIC-Jacobi and FLOSIC-KLI agree within 1%, the eigenspectrum in the FLOSIC-KLI scheme is compressed compared to FLOSIC-Jacobi. This behavior is illustrated in Fig. 7 which shows the difference between the first (lowest) and the highest occupied eigenvalues in the FLOSIC-Jacobi and FLOSIC-KLI methods. This means the core electron binding energies if estimated from the absolute eigenvalues of core electrons will differ by several eVs in the two approaches. This would also lead to differences in the prediction of the core-valence excitations used in simulating near-edge x-ray absorption fine structure (NEXAFS) spectra by two approaches.

## VI. IONIZATION POTENTIALS OF WATER CLUSTERS

We have used the present methodologies to obtain the vertical ionization potentials of water clusters from $(H_2O)_{21}$ to $(H_2O)_{30}$. The geometries of these clusters are from the recent study by Rakshit [118] and coworkers. These authors performed a large-scale search for the putative minima of



FIG. 7. The difference between the width of occupied eigenvalue spectrum (i.e., the difference in deepest $1s$ core eigenvalue and HOMO eigenvalue) (in eV) between FLOSIC-Jacobi and FLOSIC-KLI calculations.

TABLE V. HOMO and LUMO eigenvalues and HOMO-LUMO gaps (in eV) for water clusters calculated using FLOSIC-KLI.

| $H_2O$ Molecules | HOMO (eV) | | LUMO (eV) | | Gap (eV) | |
|---|---|---|---|---|---|---|
| | LDA | PBE | LDA | PBE | LDA | PBE |
| 1 | −14.75 | −14.27 | −6.30 | −5.88 | 8.45 | 8.39 |
| 5 | −14.48 | −13.95 | −6.40 | −5.87 | 8.08 | 8.07 |
| 10 | −14.11 | −13.60 | −6.84 | −6.21 | 7.27 | 7.39 |
| 15 | −14.07 | −13.56 | −7.27 | −6.59 | 6.79 | 6.96 |
| 20 | −14.49 | −13.91 | −7.03 | −6.30 | 7.46 | 7.61 |
| 21 | −13.82 | −13.31 | −7.04 | −6.35 | 6.78 | 6.96 |
| 22 | −14.44 | −13.91 | −7.17 | −6.47 | 7.27 | 7.44 |
| 23 | −13.97 | −13.49 | −7.12 | −6.44 | 6.85 | 7.05 |
| 24 | −14.24 | −13.74 | −7.21 | −6.51 | 7.03 | 7.23 |
| 25 | −14.17 | −13.63 | −7.01 | −6.28 | 7.16 | 7.35 |
| 26 | −14.08 | −13.56 | −7.18 | −6.46 | 6.90 | 7.10 |
| 27 | −14.23 | −13.75 | −7.21 | −6.51 | 7.02 | 7.24 |
| 28 | −14.25 | −13.71 | −7.27 | −6.51 | 6.98 | 7.20 |
| 29 | −14.21 | −13.68 | −7.24 | −6.50 | 6.97 | 7.18 |
| 30 | −13.97 | −13.64 | −7.45 | −6.70 | 6.51 | 6.95 |

water clusters using Monte Carlo basin paving approach with a polarizable Thole-type model for force field. These geometries were further refined at the MP2/aug-cc-pVTZ level of theory. The FLOSIC-KLI calculations were performed on the most stable water clusters at MP2/aug-cc-pVTZ level. The FODs for these clusters were obtained using the fodMC code [75]. No further optimizations of FODs were performed. To examine how well this approach works for the properties of water clusters studied herein, we optimized the FODs using the FLOSIC code for the $(H_2O)_{20}$ cluster. We find that the forces on the FODs are very small and the optimization changes the HOMO eigenvalue by 0.4%. The HOMO and the LUMO eigenvalues of water clusters along with HOMO-LUMO gap are presented in Table V. The vertical ionization potentials are the absolute values of the HOMO eigenvalues. The ionization potentials of $(H_2O)_{21}$-$(H_2O)_{30}$ water clusters are in the range 13.8 eV to 14.4 eV and do not show systematic variation with respect to size. Recently, Akter and coworkers [119] studied small water clusters using PZ-SIC and locally scaled self-interaction methods. They found that the vertical ionization potentials obtained as an absolute of the HOMO eigenvalue within the FLOSIC-LSDA scheme show systematic overestimation of approximately 2 eV when compared

with CCSD(T) ionization potentials. By adding this shift, FLOSIC-KLI ionization potentials are in good agreement with CCSD(T) energies. Likewise, the PBE FLOSIC-KLI HOMO-LUMO gaps are in the range of 6.7 eV to 7.6 eV. For the water molecule the HOMO-LUMO gap is 8.39 eV. Thus there is about a 1 to 1.4 eV reduction of the HOMO-LUMO gap from water molecule to water clusters containing 20–30 water molecules.

## VII. CONCLUSION

To summarize, we have implemented the FLOSIC method using the optimized effective potentials with the Krieger-Li-Iafrate (KLI) approximation. The implementation was tested by computing the atomic energies, atomization energies, eigenvalues and ionization potentials using standard data sets, and polarizabilities of hydrogen chains and comparing the results with those obtained using the FLOSIC-Jacobi method of Yang, Pederson, and Perdew [37]. It is found that the FLOSIC-KLI approach gives results that are in close agreement within 1%–2% of the FLOSIC-Jacobi method. We have also used the FLOSIC-KLI scheme to predict the vertical ionization energies of water clusters.

The FLOSIC-KLI is a desirable approach for larger calculations as it allows more efficient and scalable parallelization than the FLOSIC-Jacobi method. Another desirable feature of the FLOSIC-KLI approach is that it provides self-interaction-corrected virtual orbitals. The virtual orbitals are required for the calculation of excitation energies using the time-dependent density functional or for magnetic anisotropy calculations using the Pederson-Khanna method [120]. Such applications will be investigated in the future.

The data that support the findings of this study are available from the authors upon reasonable request.

## ACKNOWLEDGMENTS

[1] R. O. Jones, Density functional theory: Its origins, rise to prominence, and future, Rev. Mod. Phys. **87**, 897 (2015).

[2] J. P. Perdew and K. Schmidt, Jacob's ladder of density functional approximations for the exchange-correlation energy, in *Density Functional Theory and its Application to Materials*, edited by V. Van Doren, C. Van Alsenoy, and P. Geerlings, AIP Conf. Proc. No. 577 (AIP, New York, 2001), p. 1.

[3] M. A. Marques, M. J. Oliveira, and T. Burnus, Libxc: A library of exchange and correlation functionals for density functional theory, Comput. Phys. Commun. **183**, 2272 (2012).

[4] I. Lindgren, A statistical exchange approximation for localized electrons, Int. J. Quantum Chem. **5**, 411 (1971).

[5] M. S. Gopinathan, Improved approximate representation of the Hartree-Fock potential in atoms, Phys. Rev. A **15**, 2135 (1977).

[6] J. P. Perdew, R. G. Parr, M. Levy, and J. L. Balduz Jr., Density-Functional Theory for Fractional Particle Number: Derivative Discontinuities of the Energy, Phys. Rev. Lett. **49**, 1691 (1982).

[7] U. Lundin and O. Eriksson, Novel method of self-interaction corrections in density functional calculations, Int. J. Quantum Chem. **81**, 247 (2001).

[8] P. Mori-Sánchez, A. J. Cohen, and W. Yang, Many-electron self-interaction error in approximate density functionals, J. Chem. Phys. **125**, 201102 (2006).

[9] N. I. Gidopoulos and N. N. Lathiotakis, Constraining density functional approximations to yield self-interaction free potentials, J. Chem. Phys. **136**, 224109 (2012).

[10] D.-K. Seo, Self-interaction correction in the LDA+$U$ method, Phys. Rev. B **76**, 033102 (2007).

[11] T. Tsuneda, M. Kamiya, and K. Hirao, Regional self-interaction correction of density functional theory, J. Comput. Chem. **24**, 1592 (2003).

[12] G. Borghi, A. Ferretti, N. L. Nguyen, I. Dabo, and N. Marzari, Koopmans-compliant functionals and their performance against reference molecular data, Phys. Rev. B **90**, 075135 (2014).

[13] O. A. Vydrov and G. E. Scuseria, A simple method to selectively scale down the self-interaction correction, J. Chem. Phys. **124**, 191101 (2006).

[14] R. R. Zope, Y. Yamamoto, C. M. Diaz, T. Baruah, J. E. Peralta, K. A. Jackson, B. Santra, and J. P. Perdew, A step in the direction of resolving the paradox of Perdew-Zunger self-interaction correction, J. Chem. Phys. **151**, 214108 (2019).

[15] T. Tsuneda and K. Hirao, Self-interaction corrections in density functional theory, J. Chem. Phys. **140**, 18A513 (2014).

[16] J. C. Slater, A simplification of the Hartree-Fock method, Phys. Rev. **81**, 385 (1951).

[17] A. D. Becke, A new mixing of Hartree-Fock and local density-functional theories, J. Chem. Phys. **98**, 1372 (1993).

[18] H. Iikura, T. Tsuneda, T. Yanai, and K. Hirao, A long-range correction scheme for generalized-gradient-approximation exchange functionals, J. Chem. Phys. **115**, 3540 (2001).

[19] J. Jaramillo, G. E. Scuseria, and M. Ernzerhof, Local hybrid functionals, J. Chem. Phys. **118**, 1068 (2003).

[20] R. Baer, E. Livshits, and U. Salzner, Tuned range-separated hybrids in density functional theory, Annu. Rev. Phys. Chem. **61**, 85 (2010).

[21] J. P. Perdew and A. Zunger, Self-interaction correction to density-functional approximations for many-electron systems, Phys. Rev. B **23**, 5048 (1981).

[22] A. Ruzsinszky, J. P. Perdew, G. I. Csonka, O. A. Vydrov, and G. E. Scuseria, Density functionals that are one- and two- are not always many-electron self-interaction-free, as shown for $H_2^+$, $He_2^+$, $LiH^+$, and $Ne_2^+$, J. Chem. Phys. **126**, 104102 (2007).

[23] D. Hofmann and S. Kümmel, Self-interaction correction in a real-time Kohn-Sham scheme: Access to difficult excitations in time-dependent density functional theory, J. Chem. Phys. **137**, 064117 (2012).

[24] M. R. Pederson, R. A. Heaton, and C. C. Lin, Density-functional theory with self-interaction correction: Application to the lithium molecule, J. Chem. Phys. **82**, 2688 (1985).

[25] R. A. Heaton, J. G. Harrison, and C. C. Lin, Self-interaction correction for density-functional theory of electronic energy bands of solids, Phys. Rev. B **28**, 5992 (1983).

[26] M. R. Pederson, R. A. Heaton, and C. C. Lin, Local-density Hartree-Fock theory of electronic states of molecules with self-interaction correction, J. Chem. Phys. **80**, 1972 (1984).

[27] M. R. Pederson and C. C. Lin, Localized and canonical atomic orbitals in self-interaction corrected local density functional approximation, J. Chem. Phys. **88**, 1807 (1988).

[28] T. Körzdörfer, S. Kümmel, and M. Mundt, Self-interaction correction and the optimized effective potential, J. Chem. Phys. **129**, 014110 (2008).

[29] M. R. Pederson, A. Ruzsinszky, and J. P. Perdew, Communication: Self-interaction correction with unitary invariance in density functional theory, J. Chem. Phys. **140**, 121103 (2014).

[30] W. L. Luken and D. N. Beratan, Localized orbitals and the Fermi hole, Theor. Chem. Acc. **61**, 265 (1982).

[31] W. L. Luken and J. C. Culberson, Localized orbitals based on the Fermi hole, Theor. Chem. Acc. **66**, 279 (1984).

[32] O. A. Vydrov, G. E. Scuseria, J. P. Perdew, A. Ruzsinszky, and G. I. Csonka, Scaling down the Perdew-Zunger self-interaction correction in many-electron regions, J. Chem. Phys. **124**, 094108 (2006).

[33] Y. Yamamoto, S. Romero, T. Baruah, and R. R. Zope, Improvements in the orbitalwise scaling down of Perdew-Zunger self-interaction correction in many-electron regions, J. Chem. Phys. **152**, 174112 (2020).

[34] M. R. Pederson, Fermi orbital derivatives in self-interaction corrected density functional theory: Applications to closed shell atoms, J. Chem. Phys. **142**, 064112 (2015).

[35] M. R. Pederson and T. Baruah, Self-interaction corrections within the Fermi-orbital-based formalism, Advances in Atomic, Molecular and Optical Physics **64**, 153 (2015).

[36] D.-y. Kao and M. R. Pederson, Use of Löwdin orthogonalised Fermi orbitals for self-interaction corrections in an iron porphyrin, Mol. Phys. **115**, 552 (2017).

[37] Z.-h. Yang, M. R. Pederson, and J. P. Perdew, Full self-consistency in the Fermi-orbital self-interaction correction, Phys. Rev. A **95**, 052505 (2017).

[38] D.-y. Kao, K. Withanage, T. Hahn, J. Batool, J. Kortus, and K. Jackson, Self-consistent self-interaction corrected density functional theory calculations for atoms using Fermi-Löwdin orbitals: Optimized Fermi-orbital descriptors for Li-Kr, J. Chem. Phys. **147**, 164107 (2017).

[39] D.-y. Kao, M. Pederson, T. Hahn, T. Baruah, S. Liebing, and J. Kortus, The role of self-interaction corrections, vibrations, and spin-orbit in determining the ground spin state in a simple heme, Magnetochemistry **3**, 31 (2017).

[40] M. R. Pederson, T. Baruah, D.-y. Kao, and L. Basurto, Self-interaction corrections applied to Mg-porphyrin, $C_{60}$, and pentacene molecules, J. Chem. Phys. **144**, 164117 (2016).

[41] K. Sharkas, L. Li, K. Trepte, K. P. K. Withanage, R. P. Joshi, R. R. Zope, T. Baruah, J. K. Johnson, K. A. Jackson, and J. E. Peralta, Shrinking self-interaction errors with the Fermi-Löwdin orbital self-interaction-corrected density functional approximation, J. Phys. Chem. A **122**, 9307 (2018).

[42] R. P. Joshi, K. Trepte, K. P. K. Withanage, K. Sharkas, Y. Yamamoto, L. Basurto, R. R. Zope, T. Baruah, K. A. Jackson, and J. E. Peralta, Fermi-Löwdin orbital self-interaction correction to magnetic exchange couplings, J. Chem. Phys. **149**, 164101 (2018).

[43] A. I. Johnson, K. P. K. Withanage, K. Sharkas, Y. Yamamoto, T. Baruah, R. R. Zope, J. E. Peralta, and K. A. Jackson, The effect of self-interaction error on electrostatic dipoles calculated using density functional theory, J. Chem. Phys. **151**, 174106 (2019).

[44] J. Batool, T. Hahn, and M. R. Pederson, Magnetic signatures of hydroxyl- and water-terminated neutral and tetra-anionic $Mn_{12}$-acetate, J. Comput. Chem. **40**, 2301 (2019).

[45] J. Vargas, P. Ufondu, T. Baruah, Y. Yamamoto, K. A. Jackson, and R. R. Zope, Importance of self-interaction-error removal in density functional calculations on water cluster anions, Phys. Chem. Chem. Phys. **22**, 3789 (2020).

[46] K. Trepte, S. Schwalbe, T. Hahn, J. Kortus, D.-Y. Kao, Y. Yamamoto, T. Baruah, R. R. Zope, K. P. K. Withanage, J. E. Peralta, and K. A. Jackson, Analytic atomic gradients in the Fermi-Löwdin orbital self-interaction correction, J. Comput. Chem. **40**, 820 (2019).

[47] K. A. Jackson, J. E. Peralta, R. P. Joshi, K. P. Withanage, K. Trepte, K. Sharkas, and A. I. Johnson, Towards efficient density functional theory calculations without self-interaction: The Fermi-Löwdin orbital self-interaction correction, J. Phys.: Conf. Ser. **1290**, 012002 (2019).

[48] K. P. K. Withanage, S. Akter, C. Shahi, R. P. Joshi, C. Diaz, Y. Yamamoto, R. Zope, T. Baruah, J. P. Perdew, J. E. Peralta, and K. A. Jackson, Self-interaction-free electric dipole polarizabilities for atoms and their ions using the Fermi-Löwdin self-interaction correction, Phys. Rev. A **100**, 012505 (2019).

[49] C. Shahi, P. Bhattarai, K. Wagle, B. Santra, S. Schwalbe, T. Hahn, J. Kortus, K. A. Jackson, J. E. Peralta, K. Trepte, S. Lehtola, N. K. Nepal, H. Myneni, B. Neupane, S. Adhikari, A. Ruzsinszky, Y. Yamamoto, T. Baruah, R. R. Zope, and J. P. Perdew, Stretched or noded orbital densities and self-interaction correction in density functional theory, J. Chem. Phys. **150**, 174102 (2019).

[50] K. P. K. Withanage, K. Trepte, J. E. Peralta, T. Baruah, R. Zope, and K. A. Jackson, On the question of the total energy in the Fermi-Löwdin orbital self-interaction correction method, J. Chem. Theory Comput. **14**, 4122 (2018).

[51] K. Sharkas, K. Wagle, B. Santra, S. Akter, R. R. Zope, T. Baruah, K. A. Jackson, J. P. Perdew, and J. E. Peralta, Self-interaction error overbinds water clusters but cancels in structural energy differences, Proc. Natl. Acad. Sci. USA **117**, 11283 (2020).

[52] Y. Yamamoto, C. M. Diaz, L. Basurto, K. A. Jackson, T. Baruah, and R. R. Zope, Fermi-Löwdin orbital self-interaction correction using the strongly constrained and appropriately normed meta-GGA functional, J. Chem. Phys. **151**, 154105 (2019).

[53] S. Schwalbe, T. Hahn, S. Liebing, K. Trepte, and J. Kortus, Fermi-Löwdin orbital self-interaction corrected density functional theory: Ionization potentials and enthalpies of formation, J. Comput. Chem. **39**, 2463 (2018).

[54] S. Schwalbe, L. Fielder, J. Kraus, J. Kortus, K. Trepte, and S. Lehtola, PyFLOSIC: Python-based Fermi-Löwdin orbital self-interaction correction, J. Chem. Phys. **153**, 084104 (2020).

[55] S. Romero, Y. Yamamoto, T. Baruah, and R. R. Zope, Local self-interaction correction method with a simple scaling factor, Phys. Chem. Chem. Phys. **23**, 2406 (2021).

[56] C. M. Diaz, P. Suryanarayana, Q. Xu, T. Baruah, J. E. Pask, and R. R. Zope, Implementation of Perdew-Zunger self-interaction correction in real space using Fermi-Löwdin orbitals, J. Chem. Phys. **154**, 084112 (2021).

[57] S. Akter, Y. Yamamoto, R. R. Zope, and T. Baruah, Static dipole polarizabilities of polyacenes using self-interaction-corrected density functional approximations, J. Chem. Phys. **154**, 114305 (2021).

[58] A. Seidl, A. Görling, P. Vogl, J. A. Majewski, and M. Levy, Generalized Kohn-Sham schemes and the band-gap problem, Phys. Rev. B **53**, 3764 (1996).

[59] R. T. Sharp and G. K. Horton, A variational approach to the unipotential many-electron problem, Phys. Rev. **90**, 317 (1953).

[60] J. D. Talman and W. F. Shadwick, Optimized effective atomic central potential, Phys. Rev. A **14**, 36 (1976).

[61] J. B. Krieger, Y. Li, and G. J. Iafrate, Systematic approximations to the optimized effective potential: Application to orbital-density-functional theory, Phys. Rev. A **46**, 5453 (1992).

[62] J. Garza, J. A. Nichols, and D. A. Dixon, The optimized effective potential and the self-interaction correction in density functional theory: Application to molecules, J. Chem. Phys. **112**, 7880 (2000).

[63] S. Patchkovskii, J. Autschbach, and T. Ziegler, Curing difficult cases in magnetic properties prediction with self-interaction corrected density functional theory, J. Chem. Phys. **115**, 26 (2001).

[64] S. Patchkovskii and T. Ziegler, Phosphorus NMR chemical shifts with self-interaction free, gradient-corrected DFT, J. Phys. Chem. A **106**, 1088 (2002).

[65] X. Chu and S. I. Chu, Self-interaction-free time-dependent density-functional theory for molecular processes in strong fields: High-order harmonic generation of $H_2$ in intense laser fields, Phys. Rev. A **63**, 023411 (2001).

[66] C. Legrand, E. Suraud, and P. Reinhard, Comparison of self-interaction-corrections for metal clusters, J. Phys. B: At., Mol. Opt. Phys. **35**, 1115 (2002).

[67] S. Lehtola and H. Jónsson, Variational, self-consistent implementation of the Perdew-Zunger self-interaction correction with complex optimal orbitals, J. Chem. Theory Comput. **10**, 5324 (2014).

[68] R. R. Zope, T. Baruah, and K. A. Jackson, FLOSIC 0.2, based on the NRLMOL code of M. R. Pederson, https://flosic.org

[69] Y. Yamamoto, L. Basurto, C. M. Diaz, R. R. Zope, and T. Baruah, Self-interaction correction to density functional approximations using Fermi-Löwdin orbitals: Methodology and parallelization (unpublished).

[70] M. R. Pederson and K. A. Jackson, Variational mesh for quantum-mechanical simulations, Phys. Rev. B **41**, 7453 (1990).

[71] K. Jackson and M. R. Pederson, Accurate forces in a local-orbital approach to the local-density approximation, Phys. Rev. B **42**, 3276 (1990).

[72] D. Porezag and M. R. Pederson, Optimization of Gaussian basis sets for density-functional calculations, Phys. Rev. A **60**, 2840 (1999).

[73] J. P. Perdew, K. Burke, and M. Ernzerhof, Generalized Gradient Approximation Made Simple, Phys. Rev. Lett. **77**, 3865 (1996).

[74] J. P. Perdew and Y. Wang, Accurate and simple analytic representation of the electron-gas correlation energy, Phys. Rev. B **45**, 13244 (1992).

[75] S. Schwalbe, K. Trepte, L. Fiedler, A. I. Johnson, J. Kraus, T. Hahn, J. E. Peralta, K. A. Jackson, and J. Kortus, Interpretation and automatic generation of Fermi-orbital descriptors, J. Comput. Chem. **40**, 2843 (2019).

[76] S. Lehtola, Assessment of initial guesses for self-consistent field calculations. Superposition of atomic potentials: Simple yet efficient, J. Chem. Theory Comput. **15**, 1593 (2019).

[77] I. Ciofini, H. Chermette, and C. Adamo, A mean-field self-interaction correction in density functional theory: Implementation and validation for molecules, Chem. Phys. Lett. **380**, 12 (2003).

[78] E. Fermi and E. Amaldi, Accad. Ital. Rome **6**, 119 (1934).

[79] S. J. Chakravorty, S. R. Gwaltney, E. R. Davidson, F. A. Parpia, and C. F. Fischer, Ground-state correlation energies for atomic ions with 3 to 18 electrons, Phys. Rev. A **47**, 3649 (1993).

[80] C.-O. Almbladh and U. von Barth, Exact results for the charge and spin densities, exchange-correlation potentials, and density-functional eigenvalues, Phys. Rev. B **31**, 3231 (1985).

[81] J. P. Perdew and M. Levy, Comment on "Significance of the highest occupied Kohn-Sham eigenvalue", Phys. Rev. B **56**, 16021 (1997).

[82] A. Kramida, Yu. Ralchenko, J. Reader, and NIST ASD Team, NIST Atomic Spectra Database (ver. 5.6.1), https://physics.nist.gov/asd.

[83] L. A. Curtiss, K. Raghavachari, G. W. Trucks, and J. A. Pople, Gaussian-2 theory for molecular energies of first- and second-row compounds, J. Chem. Phys. **94**, 7221 (1991).

[84] B. J. Lynch and D. G. Truhlar, Small representative benchmarks for thermochemical calculations, J. Phys. Chem. A **107**, 8996 (2003).

[85] National Institute of Standards and Technology, NIST Computational Chemistry Comparison and Benchmark Database, http://cccbdb.nist.gov

[86] S. J. A. van Gisbergen, P. R. T. Schipper, O. V. Gritsenko, E. J. Baerends, J. G. Snijders, B. Champagne, and B. Kirtman, Electric Field Dependence of the Exchange-Correlation Potential in Molecular Chains, Phys. Rev. Lett. **83**, 694 (1999).

[87] O. V. Gritsenko, S. J. A. van Gisbergen, P. R. T. Schipper, and E. J. Baerends, Origin of the field-counteracting term of the Kohn-Sham exchange-correlation potential of molecular chains in an electric field, Phys. Rev. A **62**, 012507 (2000).

[88] P. Mori-Sánchez, Q. Wu, and W. Yang, Accurate polymer polarizabilities with exact exchange density-functional theory, J. Chem. Phys. **119**, 11001 (2003).

[89] B. Kirtman, S. Bonness, A. Ramirez-Solis, B. Champagne, H. Matsumoto, and H. Sekino, Calculation of electric dipole (hyper) polarizabilities by long-range-correction scheme in density functional theory: A systematic assessment for polydiacetylene and polybutatriene oligomers, J. Chem. Phys. **128**, 114108 (2008).

[90] J. Vargas, M. Springborg, and B. Kirtman, Electronic responses of long chains to electrostatic fields: Hartree-Fock vs. density-functional theory: A model study, J. Chem. Phys. **140**, 054117 (2014).

[91] T. Aschebrock and S. Kümmel, Ultranonlocality and accurate band gaps from a meta-generalized gradient approximation, Phys. Rev. Res. **1**, 033082 (2019).

[92] S. Kummel, L. Kronik, and J. P. Perdew, Electrical Response of Molecular Chains from Density Functional Theory, Phys. Rev. Lett. **93**, 213002 (2004).

[93] H. Sekino, Y. Maeda, and M. Kamiya, Influence of the long-range exchange effect on dynamic polarizability, Mol. Phys. **103**, 2183 (2005).

[94] R. Baer and D. Neuhauser, Density Functional Theory with Correct Long-Range Asymptotic Behavior, Phys. Rev. Lett. **94**, 043002 (2005).

[95] C. D. Pemmaraju, T. Archer, D. Sánchez-Portal, and S. Sanvito, Atomic-orbital-based approximate self-interaction correction scheme for molecules and solids, Phys. Rev. B **75**, 045101 (2007).

[96] A. Ruzsinszky, J. P. Perdew, G. I. Csonka, G. E. Scuseria, and O. A. Vydrov, Understanding and correcting the self-interaction error in the electrical response of hydrogen chains, Phys. Rev. A **77**, 060502(R) (2008).

[97] N. T. Maitra and M. Van Faassen, Improved exchange-correlation potential for polarizability and dissociation in density functional theory, J. Chem. Phys. **126**, 191106 (2007).

[98] T. Körzdörfer, M. Mundt, and S. Kümmel, Electrical Response of Molecular Systems: The Power of Self-Interaction Corrected Kohn-Sham Theory, Phys. Rev. Lett. **100**, 133004 (2008).

[99] J. Messud, Z. Wang, P. M. Dinh, P.-G. Reinhard, and E. Suraud, Polarizabilities as a test of localized approximations to the self-interaction correction, Chem. Phys. Lett. **479**, 300 (2009).

[100] J. F. Janak, Proof that $\frac{\delta E}{\delta n_i} = \varepsilon$ in density-functional theory, Phys. Rev. B **18**, 7165 (1978).

[101] M. Levy, J. P. Perdew, and V. Sahni, Exact differential equation for the density and ionization energy of a many-particle system, Phys. Rev. A **30**, 2745 (1984).

[102] P. Politzer and F. Abu-Awwad, A comparative analysis of Hartree-Fock and Kohn-Sham orbital energies, Theor. Chem. Acc. **99**, 83 (1998).

[103] R. Stowasser and R. Hoffmann, What do the Kohn-Sham orbitals and eigenvalues mean? J. Am. Chem. Soc. **121**, 3414 (1999).

[104] D. P. Chong, O. V. Gritsenko, and E. J. Baerends, Interpretation of the Kohn-Sham orbital energies as approximate vertical ionization potentials, J. Chem. Phys. **116**, 1760 (2002).

[105] M. Grüning, A. Marini, and A. Rubio, Density functionals from many-body perturbation theory: The band gap for semiconductors and insulators, J. Chem. Phys. **124**, 154108 (2006).

[106] A. J. Cohen, P. Mori-Sánchez, and W. Yang, Fractional charge perspective on the band gap in density-functional theory, Phys. Rev. B **77**, 115123 (2008).

[107] A. M. Teale, F. De Proft, and D. J. Tozer, Orbital energies and negative electron affinities from density functional theory: Insight from the integer discontinuity, J. Chem. Phys. **129**, 044110 (2008).

[108] P. Mori-Sánchez, A. J. Cohen, and W. Yang, Localization and Delocalization Errors in Density Functional Theory and Implications for Band-Gap Prediction, Phys. Rev. Lett. **100**, 146401 (2008).

[109] W. Yang, A. J. Cohen, and P. Mori-Sánchez, Derivative discontinuity, bandgap and lowest unoccupied molecular orbital in density functional theory, J. Chem. Phys. **136**, 204111 (2012).

[110] L. Kronik, T. Stein, S. Refaely-Abramson, and R. Baer, Excitation gaps of finite-sized systems from optimally tuned range-separated hybrid functionals, J. Chem. Theory Comput. **8**, 1515 (2012).

[111] E. J. Baerends, O. V. Gritsenko, and R. Van Meer, The Kohn-Sham gap, the fundamental gap and the optical gap: The physical meaning of occupied and virtual Kohn-Sham orbital energies, Phys. Chem. Chem. Phys. **15**, 16408 (2013).

[112] R. Van Meer, O. V. Gritsenko, and E. J. Baerends, Physical meaning of virtual Kohn-Sham orbitals and orbital energies: An ideal basis for the description of molecular excitations, J. Chem. Theory Comput. **10**, 4432 (2014).

[113] J. P. Perdew, W. Yang, K. Burke, Z. Yang, E. K. Gross, M. Scheffler, G. E. Scuseria, T. M. Henderson, I. Y. Zhang, A. Ruzsinszky, H. Peng, J. Sun, E. Trushin, and A. Görling, Understanding band gaps of solids in generalized Kohn-Sham theory, Proc. Natl. Acad. Sci. USA **114**, 2801 (2017).

[114] J. P. Perdew and A. Ruzsinszky, Density-functional energy gaps of solids demystified, Eur. Phys. J. B **91**, 108 (2018).

[115] E. J. Baerends, Density functional approximations for orbital energies and total energies of molecules and solids, J. Chem. Phys. **149**, 054105 (2018).

[116] E. J. Baerends, On derivatives of the energy with respect to total electron number and orbital occupation numbers. A critique of Janak's theorem, Mol. Phys. **118**, e1612955 (2020).

[117] R. W. Godby and R. J. Needs, Metal-Insulator Transition in Kohn-Sham Theory and Quasiparticle Theory, Phys. Rev. Lett. **62**, 1169 (1989).

[118] A. Rakshit, P. Bandyopadhyay, J. P. Heindel, and S. S. Xantheas, Atlas of putative minima and low-lying energy networks of water clusters $n = 3$–25, J. Chem. Phys. **151**, 214307 (2019).

[119] S. Akter, Y. Yamamoto, C. M. Diaz, K. A. Jackson, R. R. Zope, and T. Baruah, Study of self-interaction errors in density functional predictions of dipole polarizabilities and ionization energies of water clusters using Perdew-Zunger and locally scaled self-interaction corrected methods, J. Chem. Phys. **153**, 164304 (2020).

[120] M. R. Pederson and S. N. Khanna, Magnetic anisotropy barrier for spin tunneling in $Mn_{12}O_{12}$ molecules, Phys. Rev. B **60**, 9566 (1999).